Chem

Article

Rapid access to 3-substituted bicyclo[1.1.1] pentanes

Graphical abstract

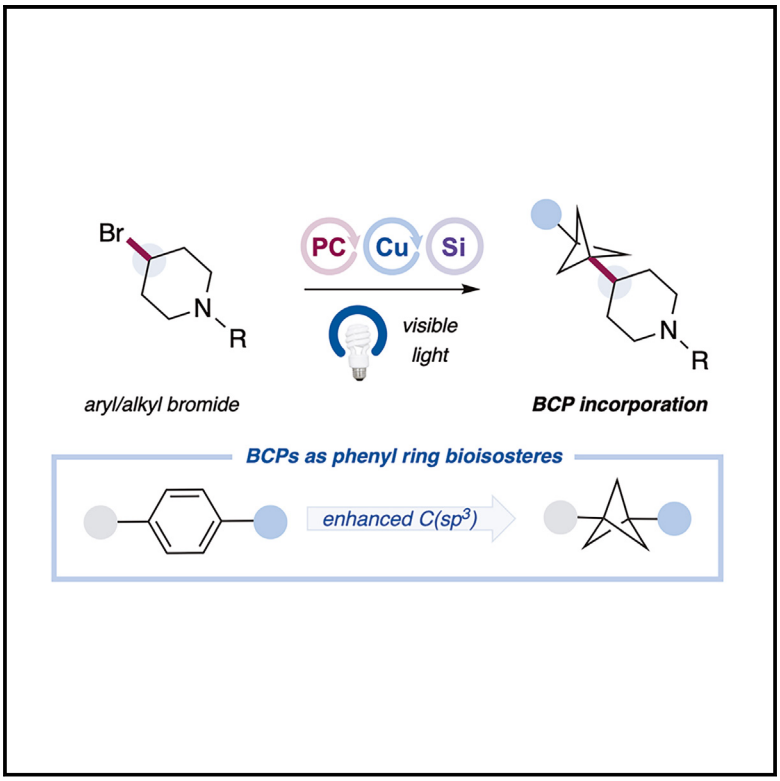

Authors

Katherine I. Burton, David W.C. MacMillan

Correspondence

dmacmill@princeton.edu

In brief

Growing interest in C(sp^3)-rich bioisosteres has driven efforts to synthetically manipulate bicyclo[1.1.1] pentane (BCP) scaffolds. The strained geometry of BCPs imparts high C(sp^3)–H bond-dissociation energies that enhance the metabolic stability of the carbocycle. However, quaternary 3-alkylated BCPs remain underdeveloped as bioisosteres of benzylic environments. The reported method enables access to 3-alkylated and 3-arylated BCPs under mild photoredox conditions by using commercially abundant precursors.

Highlights

- Mild photoredox conditions afford 3-substituted BCP products
- Method furnishes diverse C(sp^3)-rich alkyl and aryl chemical space
- Rapid access to BCP motifs bearing three and four quaternary centers

Burton & MacMillan, 2025, Chem *11*, 102537
May 8, 2025
https://doi.org/10.1016/j.chempr.2025.102537

CellPress

Please cite this article in press as: Burton and MacMillan, Rapid access to 3-substituted bicyclo[1.1.1]pentanes, Chem (2025), https://doi.org/10.1016/j.chempr.2025.102537

Chem

CellPress

Article

Rapid access to 3-substituted bicyclo[1.1.1]pentanes

Katherine I. Burton[1] and David W.C. MacMillan[1,2,*]
[1]Merck Center for Catalysis at Princeton University, Princeton, NJ 08544, USA
[2]Lead contact
*Correspondence: dmacmill@princeton.edu
https://doi.org/10.1016/j.chempr.2025.102537

THE BIGGER PICTURE Visible-light-mediated metallaphotoredox catalysis has emerged as an effective strategy for the generation of high-energy species from commercially abundant precursors. The capacity to bypass harsh organometallic transfer reagents and volatile chemicals further heightens the potential utility of photoredox platforms. Recently, bicyclo[1.1.1]pentane (BCP) carbocycles have gained prominence as aryl-ring bioisosteres because of the clinical benefits of incorporating enhanced F(sp^3) environments into drug design. The strained rigidity of BCPs simultaneously imparts metabolic stability while promoting the configurational retention of substituted aryl-ring exit vectors. We report an operationally trivial, metallaphotoredox-based method that achieves 3-alkylation and 3-arylation of BCP linchpins by using abundant, bench-stable feedstocks. With high functional-group compatibility and amenability to drug motifs, this strategy enables modular BCP synthesis. We anticipate that these developments will provide access to greater substrate diversity, including motifs that cannot be readily accessed via conventional closed-shell methods.

SUMMARY

The prevalence of benzene rings in pharmaceutical scaffolds has prompted efforts to identify structural bioisosteres with improved *in vivo* properties. Notably, investigators have leveraged bicyclo[1.1.1]pentanes (BCPs)—C(sp^3)-enriched, 1,4-disubstituted phenyl bioisosteres—to tune the pharmacokinetic profiles of lead compounds. Although 3-arylated BCPs have been widely implemented to confer resistance to oxidative degradation and hydrogen atom transfer (HAT) processes, the analogous 3-alkylated BCPs remain underexplored as bioisosteric "benzylic" C–H motifs. Current methods for installing 3-alkylated BCP motifs are heavily reliant on lengthy *de novo* synthesis and the preparation of reactive [1.1.1]propellane feedstocks, limiting their adoption in drug-discovery programs. In this report, we disclose a mild, unified method for the preparation of both alkyl- and aryl-substituted BCPs from bench-stable precursors. This method, which proceeds via dual copper-photoredox catalysis, is capable of installing BCP functionalities onto a range of saturated motifs, aryl-containing residues, and medicinally relevant heterocycles.

INTRODUCTION

The selective tuning of absorption, distribution, metabolism, and excretion-toxicity (ADMET) properties is a critical component of drug design. Notably, incorporating a higher fraction of sp^3-hybridized atoms (Fsp^3) leads to improved solubility,[1] reduced off-target binding promiscuity, and enhanced likelihood of clinical success.[2,3] The strategic installation of Fsp^3-rich bioisosteres can permit selective modulation of pharmacokinetic profiles while retaining physiological efficacy.[4–6] Arenes are prevalent in pharmaceuticals, yet oxidative degradation pathways can lead to *in vivo* toxicity while promoting rapid metabolic excretion.[7] Judicious evaluation of both bioavailability and drug stability is critical for tuning the therapeutic index of a lead candidate.[8] Accordingly, the selective incorporation of 3-substituted bicyclo[1.1.1]pentanes (BCPs) as 1,4-disubstituted phenyl ring bioisosteres has been shown to improve the thermodynamic solubility of parent molecules while suppressing oxidative metabolism.[9,10] Because of their rigid geometry and consequently inert aliphatic C–H bonds, 3-substituted BCPs recapitulate the geometric exit vectors exhibited in *para*-substituted aryl rings (Scheme 1, top).[11] We propose that quaternized 3-alkylated BCPs could offer synthetic access to stabilized bioisosteric pseudo-"benzylic" environments that would otherwise present metabolic weak points in a traditional aryl scaffold (see supplemental information sections S2 and S2 and Table S1). Several recently reported, elegant C(sp^2) installation strategies include carbene insertion,[12] atom-transfer radical addition (ATRA),[13,14] and strain-release paradigms.[15–19] However, the incorporation of tertiary C(sp^3) functionalization remains synthetically challenging and heavily reliant on the preparation of [1.1.1]propellane or pre-activation strategies.[20–22] Furthermore, established methods can face challenges with functional-group

Please cite this article in press as: Burton and MacMillan, Rapid access to 3-substituted bicyclo[1.1.1]pentanes, Chem (2025), https://doi.org/10.1016/j.chempr.2025.102537

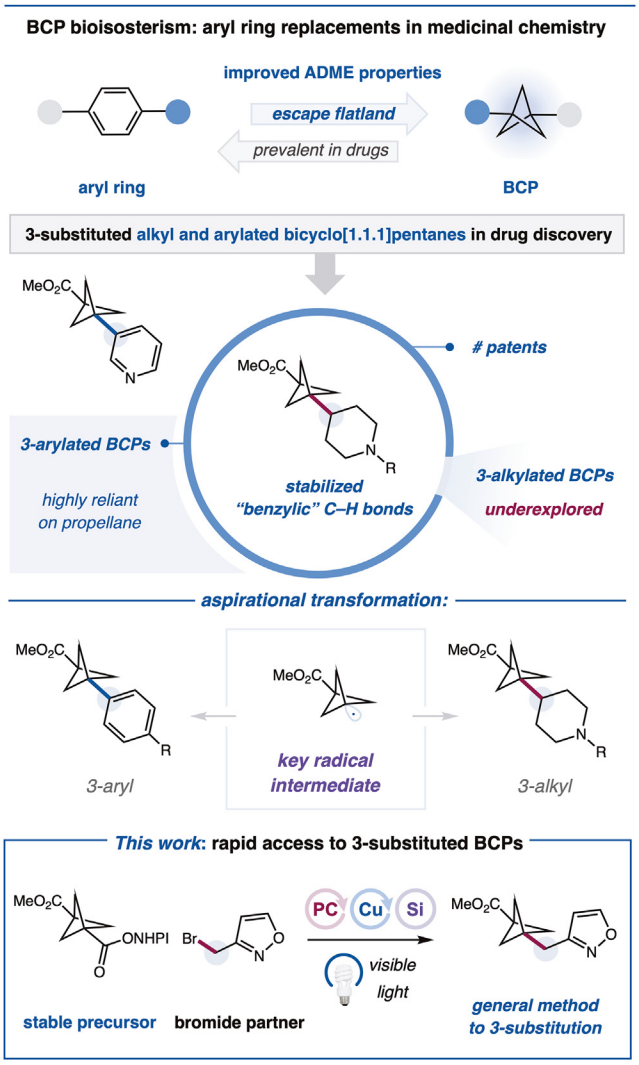

Scheme 1. Bicyclo[1.1.1]pentanes as phenyl bioisosteres

compatibility because they require harsh conditions and reactive precursors. Consequently, late-stage BCP incorporation frequently requires *de novo* synthesis and multistep re-routes, ultimately severely affecting the total number of industrial patents encompassing alkylated BCP motifs (Figure 1, middle).[23,24]

We aimed to address this outstanding challenge by developing a mild coupling platform capable of delivering a diverse array of both 3-alkylated or 3-arylated BCPs in a single-step, one-flask protocol. To this end, we were inspired by *N*-hydroxyphthalimide (NHPI) redox-active ester-functionalized BCPs as attractive, bench-stable alternatives to reactive propellane feedstocks (Scheme 1, bottom).[25–29] The reported transformation seeks to expand on prior methods by introducing a modular platform capable of selective site functionalization, which should prove useful for late-stage installation of drug motifs without relying on stoichiometric zinc or Hantzsch ester reductants, organolithium, Grignard, or reactive strain-release reagents.[30–33] We report an expansion of accessible chemical space via rapid access to alkyl bromides—a underexplored challenge. The method is designed to satisfy three key goals:

(1) Obviate the reliance on stoichiometric metal reagents. Prior art relies extensively on organometallics as coupling partners and stochiometric metals (e.g., Zn) as reductants. In the interest of improving functional-group compatibility and accessing more diverse chemical space, the current method uses neither.
(2) Circumvent the reliance on [1.1.1]propellane for 3-functionalization. The necessary calibration of [1.1.1]propellane stock solutions to monitor precursor decomposition offers the potential for improvement in any coupling regime.
(3) Deliver access to greater chemical space alongside improved synthetic modularity. This method does not rely on strain release to achieve 3-functionalization and therefore seeks to enable sequential or late-stage functionalization.

RESULTS AND DISCUSSION

Reaction development

At the outset, we focused on developing a BCP 3-functionalization method centered on a platform of convenience and modularity. Traditional methods require that [1.1.1]propellane be prepared from organolithium reagents and distilled immediately prior to use. By contrast, we envisioned employing one universal, bench-stable building block amenable to diverse functionalization. Specifically, the activated BCP acid (Scheme 2, structure **9**) was viewed as a convenient precursor for radical generation.

Transition-metal-catalyzed alkyl-alkyl cross-couplings have traditionally been beset by multiple challenges, including competitive β-hydride elimination and sluggish elementary activation steps.[34] Circumventing strain-release or multistep paradigms to access 3-alkylation was a particular consideration given that traditional nickel-mediated routes offer restrictive access to aromatic or sp^2 coupling partners. To bypass these obstacles, we envisioned harnessing copper as a broadly tolerant catalytic platform able to undergo kinetically facile reductive elimination predisposed toward C(sp^2)– and C(sp^3)–BCP bond formation. Copper-mediated cross-coupling reactions traditionally rely on air- and moisture-sensitive transmetalation reagents to overcome a kinetically challenging oxidative addition step.[35,36] To avoid using these sensitive organolithium and Grignard reagents, which can present challenges in late-stage settings, we opted to employ a mild photocatalytic platform to unveil the radical coupling partners from abundant halide precursors. We chose to utilize readily available alkyl bromides instead of the more expensive, reductively labile alkyl iodide precursors. (Furthermore, a challenging alkyl bromide reduction [$E_{1/2}$ = −2.5 V vs. saturated calomel electrode (SCE)] and high bond strength [bond-dissociation energy ~ 70–80 kcal mol^{-1}] prevent off-target reactivity.) To this end, our laboratory previously disclosed the use of open-shell silicon reagents to selectively activate organohalides via a polarity-matched halogen atom transfer (XAT) event.[37,38] This XAT event would be expected to proceed on orders greater than k ~ 10^6 $M^{-1}s^{-1}$ to provide the key alkyl radical species.[39–41] Crucially, using an aminosilane reagent

Please cite this article in press as: Burton and MacMillan, Rapid access to 3-substituted bicyclo[1.1.1]pentanes, Chem (2025), https://doi.org/10.1016/j.chempr.2025.102537

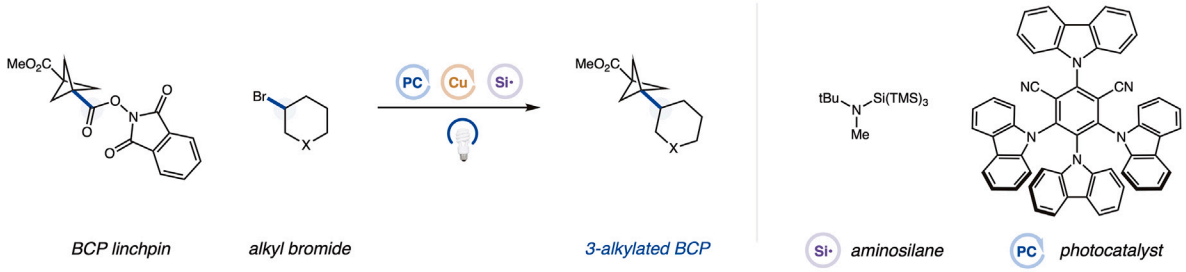

primary bromides

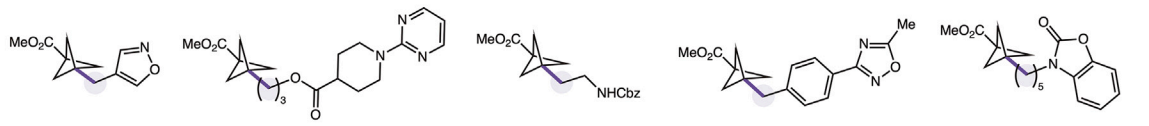

14, 46% yield

15, 56% yield

16, 56% yield

17, 57% yield

18, 50% yield

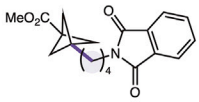

19, 53% yield

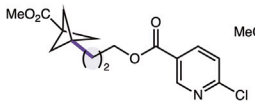

20, 50% yield

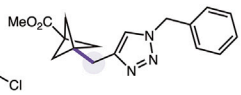

21, 57% yield

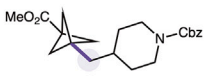

22, 52% yield

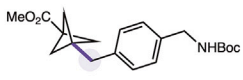

23, 48% yield

secondary bromides

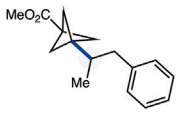

24, 72% yield

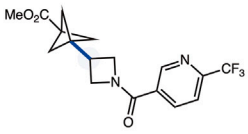

25, 63% yield[a]

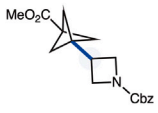

26, 51% yield

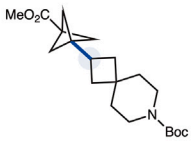

27, 40% yield

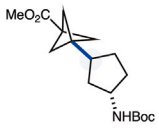

(±) **28**, 50% yield[b]

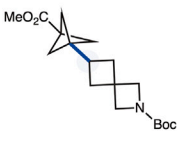

29, 30% yield

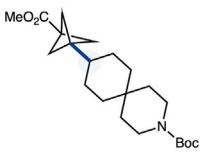

30, 54% yield

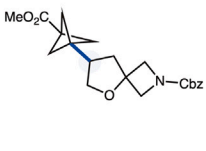

31, 59% yield

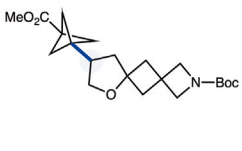

32, 58% yield

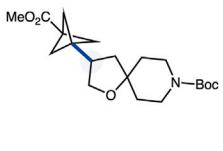

33, 70% yield[c]

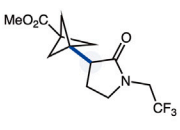

34, 50% yield

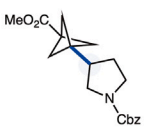

35, 60% yield

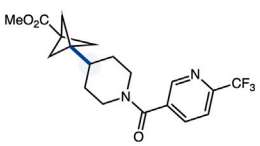

36, 63% yield

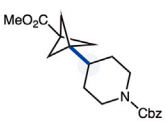

37, 54% yield

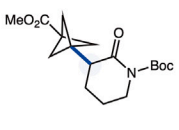

38, 49% yield

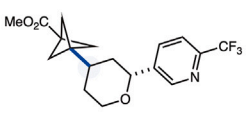

39, 54% yield[d]

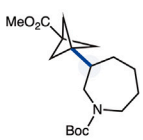

40, 42% yield

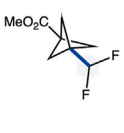

41, 42% yield[e]

tertiary bromide

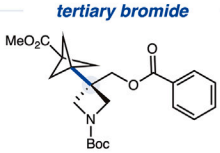

42, 31% yield

See Supporting Information for additional examples

(legend on next page)

Please cite this article in press as: Burton and MacMillan, Rapid access to 3-substituted bicyclo[1.1.1]pentanes, Chem (2025), https://doi.org/10.1016/j.chempr.2025.102537

would allow us to simultaneously sidestep the reliance on harsh (e.g., Zn) reductants while achieving mild access to the desired XAT event. Next, a reductive pathway would achieve photocatalyst (PC) turnover and concurrently unveil the BCP bridgehead radical, capable of being captured by the copper catalyst.[42]

The proposed reaction mechanism is outlined in Scheme 2. PC **1** (2,4,5,6-tetrakis(9H-carbazol-9-yl)isophthalonitrile [4CzIPN]) accesses a long-lived, triplet excited state under blue-light irradiation (τ = 5.1 s, $E_{1/2}$ = +1.35 V vs. SCE in MeCN).[38] The excited state, **2**, is reduced by aminosilane reagent **4** to generate **3**, which undergoes single-electron reduction (SET) of NHPI-functionalized BCP ester **9** to promote the decarboxylative formation of radical **10** while regenerating PC **1** and 1 equiv of phthalimide anion. The activation of $CuBr_2$ (**11a**) is feasible under this PC regime ($E_{1/2}$ [4CzIPN/4CzIPN^{-}•= −1.21 V vs. SCE]) and affords Cu(I) species **11b**. Intermediate **10** is postulated to undergo radical trapping into copper catalyst **11b** to afford Cu(II)–BCP intermediate **12**. Simultaneously, the oxidative activation of aminosilane reagent **4** is hypothesized to furnish radical cation **5**, which undergoes base-mediated substitution at silicon and α-trimethylsilyl group migration to unveil nucleophilic silyl radical **6**.[43] A polarity-matched XAT event with unactivated alkyl bromide **7** liberates 1 equiv of carbon-centered radical **8**. Subsequent radical trapping is postulated to occur at near diffusion-controlled rates ($k \sim 10^9$ $M^{-1}s^{-1}$) to furnish Cu(III) intermediate **13**.[44] A favorable inner-sphere reductive elimination is proposed to promote bond formation, regenerating catalytically active Cu(I) while delivering the target 3-substituted BCP product.

Extensive optimization studies revealed that combining alkyl bromide with *tert*-butyl-methyl-aminosilane reagent **4** (2.0 equiv), NHPI-BCP **9** (1.5 equiv), $CuBr_2$ (20 mol %), sodium acetate (2.0 equiv), and 4CzIPN (1 mol %), followed by subsequent irradiation in the presence of acetone (0.05 M), furnished the desired product in optimal yield (Figure S26). Further studies revealed that higher PC loadings (10 mol % 4CzIPN) could furnish product **36** in 78% yield (see the supplemental information). As expected, no product was observed in the absence of silane, PC, or light (see Figure S18 for control studies). We hypothesized that successful execution of the proposed transformation would require careful control of the relative rates of the XAT and decarboxylation steps. We recognize that tuning the relative rates of radical generation is critical for achieving efficient Cu speciation and therein attaining a kinetically favorable reductive elimination while minimizing unproductive pathways.[45] Accordingly, the competing protodehalogenation and homodimerization byproducts were ultimately suppressed via the attenuation of silane equivalencies and copper catalyst loading.

With optimal conditions in hand, we sought to examine the alkylation scope for this transformation (Figure 1). We were delighted to find that a variety of unactivated primary bromides were well tolerated (**14**–**23**, 46%–57% yield). The mild reaction conditions enabled extension of this platform to drug core moieties,[46] furnishing a BCP-functionalized isoxazole derivative (**14**, 46% yield) and protected aminopyrimidine (**15**, 56% yield) in synthetically useful yields. Further, the protocol enabled direct access to β-amino pharmaceutical derivatives, as exemplified by the phenethylamine bioisostere (**16**, 56% yield). We also observed that the rapid incorporation of the BCP scaffold into medicinally relevant heterocycles generated oxadiazole (**17**, 57% yield). This protocol further permitted the incorporation of the BCP bioisostere into the 2-benzoxazolone core of FDA-approved pharmaceutical chlorzoxazone (**18**, 50% yield). The incorporation of synthetically relevant linchpins for post-derivatization was demonstrated via a primary amine surrogate (**19**, 53% yield) and pendant pyridyl chloride (**20**, 50% yield). Given the diverse pharmaceutical profile of triazoles and their use in antifungal agents,[47] we were pleased to demonstrate the compatibility of this net redox-neutral method with a triazole functionality (**21**, 57% yield). As an extension of this platform, we next evaluated C–C bond formation between the BCP carbocycle (strain energy $\sim$ 65–68 kcal mol^{-1})[48] and strained coupling partners. We were delighted to note the translatability between secondary acyclic (**24**, 72% yield) and cyclic (**25**, 63% yield) environments. We further demonstrated the compatibility of a diverse range of electronically and topologically differentiated secondary bromide substrates (**24**–**41**, 30%–72% yield). A collective desire to increase F(sp^3) character has prompted growing interest in spirocyclic scaffolds, the three dimensionality of which helps to suppress off-target binding promiscuity in late-stage drug candidates.[49] We sought to investigate the compatibility of alkyl spirocyclic coupling partners in our method. We generated a library of previously undocumented BCP-coupled carbocyclic motifs, including select permutations of 4,6- (**27**, 40% yield), 4,4- (**29**, 30% yield), 6,6- (**30**, 54% yield), 5,4- (**31**, 59% yield), and 5,6- (**33**, 70% yield) spirocycles. These efforts yielded a diverse range of BCP structural motifs bearing three and four quaternary centers. Moreover, we successfully synthesized scaffold **32** (58% yield) to access a tetracyclic BCP motif.

Recognizing the prevalence of piperidine motifs across diverse pharmaceutical classes,[50] we were gratified to observe the streamlined incorporation of BCP bioisosteres into these scaffolds (**36**, 63% yield; **37**, 54% yield). To explore the limits of functional-group compatibility, we further tested this methodology on substrates bearing stereochemical information. Thus, nitrogen-functionalized compound **28** was accessed in 50% yield, and further exploration of chemical space furnished

Figure 1. Alkyl bromide scope for copper-catalyzed 3-alkylation of BCP bioisostere

Reactions were performed with alkyl bromide (1 equiv), BCP linchpin (1.5 equiv), *t*BuMeNSi(TMS)$_3$ (2.0 equiv), $CuBr_2$ (0.2 equiv), NaOAc (2.00 equiv), and 4CzIPN (1 mol %) in acetone (0.05 M) under integrated photoreactor irradiation (450 nm) for 0.5 h unless otherwise indicated. All yields are isolated unless otherwise noted. See the supplemental information for experimental details.

[a]Performed with 2 mol % 4CzIPN.

[b]Isolated as an inseparable mixture of diastereomers.

[c]Assay yield determined by ^{1}H NMR analysis using mesitylene as the internal standard.

[d](2.33:1) d.r. (determined by NMR); the target was isolated as the acid.

[e]Irradiation performed for 2 h; assay yield was determined by ^{19}F NMR analysis using 1,4-difluorobenzene as the internal standard.

Please cite this article in press as: Burton and MacMillan, Rapid access to 3-substituted bicyclo[1.1.1]pentanes, Chem (2025), https://doi.org/10.1016/j.chempr.2025.102537

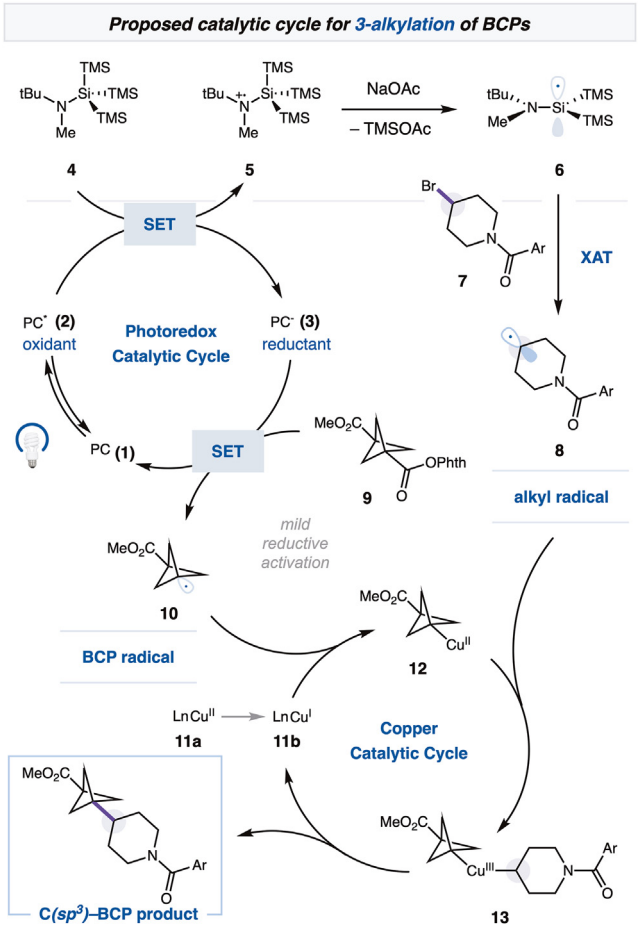

Scheme 2. Plausible mechanism of the proposed transformation

tetrahydropyran scaffold **39** in 54% yield (2.33:1 d.r.). We next pursued α-bromo amides (**34**, 50% yield; **38**, 49% yield) to demonstrate the compatibility of electron-deficient radicals with this method. Finally, the platform was amenable to tertiary bromide substrates, furnishing contiguous quaternary centers in synthetically useful yield (**42**, 31% yield).

Despite their prevalence in approved small-molecule drugs, phenols are susceptible to rapid excretion because of their hydroxylated cores.[51] Difluoromethyl functionalities have been harnessed as bioisosteres of alcohol groups, partly because of their advantageous retention of hydrogen-bonding activity.[52] Consequently, we sought to access phenol bioisosteres by extending our BCP protocol to difluoromethylation. We were pleased to find that the desired adduct, **41**, was accessed in 42% assay yield in a single step from simple starting materials.

Extension of reaction design to incorporate (hetero)aryl halides

Flat, sp^2-rich environments are pervasive in drug discovery[2,53] as a result of the prevalence of robust synthetic strategies (such as Suzuki-Miyaura couplings) that facilitate rapid C(sp^2) fragment installation.[54] By contrast, the synthetic challenges associated with incorporating three dimensionality into drug scaffolds have limited expansion in this area. Consequently, we sought to devise a single platform capable of accessing both alkylated and arylated BCPs to furnish bioisosteres of biaryl environments. We envisioned that a broadly tolerant, modular platform for constructing BCP motifs would potentially accelerate the design of new drug analogs.

To this end, we were pleased to find that BCPs could be appended to an array of electronically diverse aryl and heteroaryl bromides under modified conditions (Figure 2; 43–59, 40%–66% yields). Notably, these conditions enabled facile 3-arylation without the need for organogrignards, [1.1.1]propellane, or forcing conditions (see the supplemental information for further details).[27] Given the value of fluorine motifs in drug discovery,[55] we were delighted to observe that trifluoromethyl groups were tolerated in the reaction conditions (**43**, 52% yield). Further, we successfully incorporated cross-coupling partners for post-functionalization (**44**, 50% yield), opening avenues to downstream diversification. In line with this logic, nitrile-substituted scaffolds (**45**, 57% yield; **46**, 52% yield; **48**, 50% yield) offer synthetic handles for downstream redox manipulations. In investigating the effects of strain in drug-relevant architectures, we observed that incorporating cyclopropyl groups can correlate with improved drug-candidate progression from preclinical to clinical-phase trials.[56] Accordingly, we were gratified to find that cyclopropane exit vectors were tolerated under the reported method (**46**, 52% yield; **47**, 41% yield). We next investigated a series of medicinally relevant heterocycles (**49**–**59**, 40%–66% yields) by particularly focusing on pharmaceutically privileged nitrogen-containing structures. We accessed varied aryl substitution patterns, including electron-deficient pyridyl motifs (**49**–**56**, 40%–66% yield), quinoxaline scaffolds (**57**, 43% yield), phthalide (**58**, 42% yield), and pyrazolo-pyridines (**59**, 49% yield; see the supplemental information for additional examples, specifically section S7 and Figures S26–S32 for an example inspired by an industrial patent).

Incorporation of drug-relevant motifs

Finally, we examined the applicability of the method to the incorporation of drug-like motifs (Figure 3). Encouraged by an operationally facile functionalization of the quinolinone core of the antipsychotic aripiprazole (**60**, 64% yield), we next accessed a tafamidis analog (**61**, 50% yield). We achieved the direct functionalization of the commercially available antifungal bromuconazole in a synthetically useful yield (**62**, 32% yield), alongside the synthesis of BCP-functionalized 6-chloropyridazine (**63**, 51% yield). These results collectively demonstrate that our operationally streamlined approach tolerates a variety of complex, densely functionalized heterocycles bearing aryl halides and alternate synthetic handles. To probe the translatability of this method to alternate bioisosteric environments, we modified the arylation conditions by using an oxa-bicyclo[2.1.1]hexane redox-active ester fragment to attain product in 42% yield vs. 1,4-difluorobenzene (see Figure S27 for details).

Conclusion

In conclusion, we have demonstrated the rapid incorporation of 3-substituted BCPs into diverse alkyl and (hetero)aryl coupling

Please cite this article in press as: Burton and MacMillan, Rapid access to 3-substituted bicyclo[1.1.1]pentanes, Chem (2025), https://doi.org/10.1016/j.chempr.2025.102537

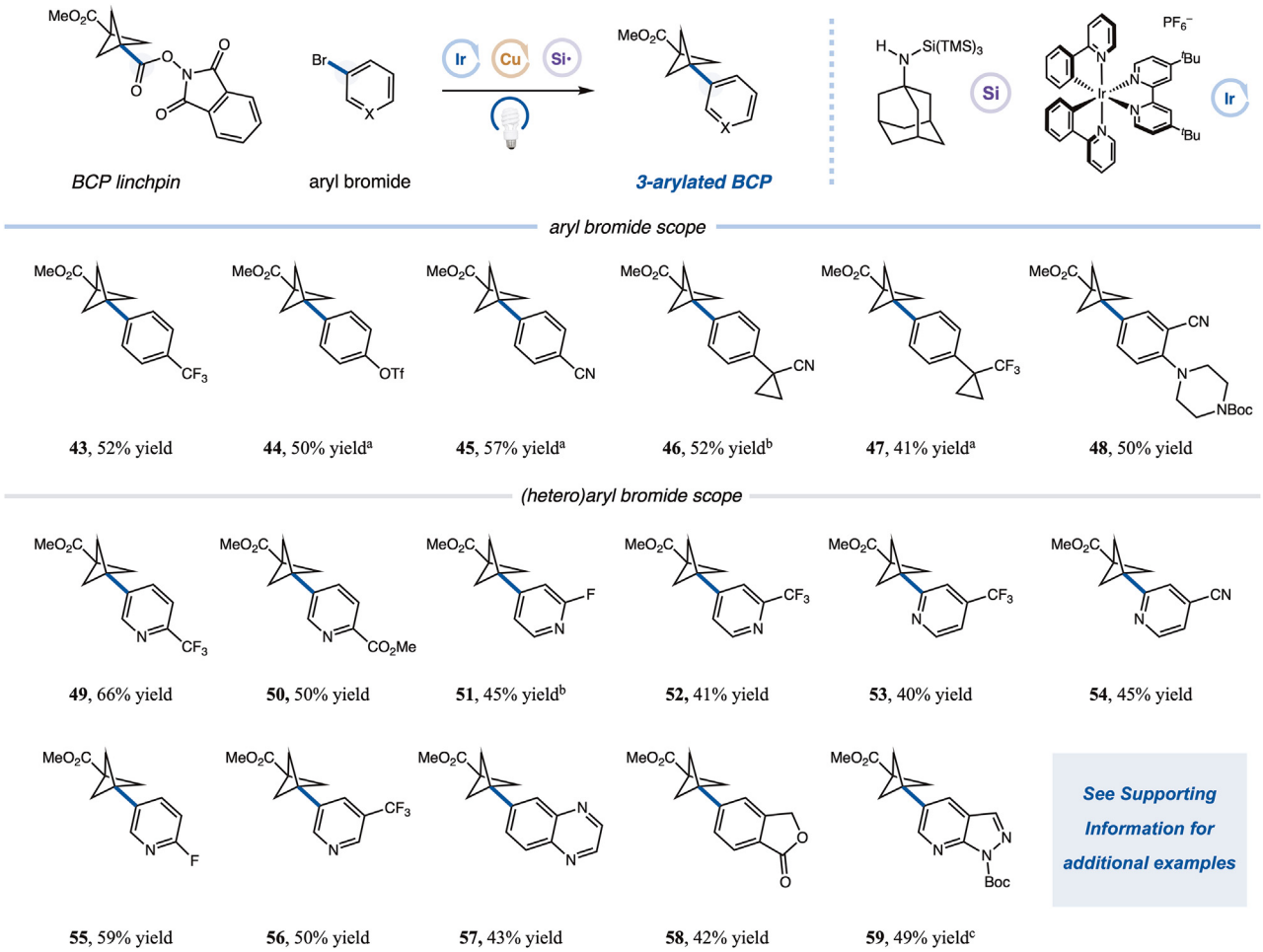

Figure 2. Aryl bromide scope for copper-catalyzed 3-(hetero)arylation of BCP bioisostere

Reactions were performed with aryl bromide (1 equiv), BCP linchpin (3.2 equiv), $AdHNSi(TMS)_3$ (2.0 equiv), $Cu(TMHD)_2$ (0.5 equiv), $[Ir(dtbppy)(ppy)_2][PF_6]$ (1 mol %), and NaOAc (8.00 equiv) in acetone (0.05 M) under integrated photoreactor irradiation (450 nm) for 1 h unless otherwise indicated. All yields are isolated unless otherwise noted. See the supplemental information for experimental details and the standard (hetero)arylation method.

[a]Assay yields determined by ^1H NMR analysis using mesitylene as the internal standard after silica gel chromatography.

[b]Prepared with lower (1.5 equiv) BCP linchpin loading.

[c]Isolated as a mixture of Boc-deprotected product.

partners via the implementation of a bench-stable BCP precursor under mild metallaphotoredox conditions. This coupling protocol is operationally robust and broadly tolerant to a variety of substrate electronics. We have shown that the mild conditions of the reported procedure allow broad functional-group compatibility and enable late-stage functionalization of drug scaffolds, with a particular focus on diversely strained alkyl environments. We anticipate that these findings will aid in the continued exploration of BCP bioisosteres in complex, drug-like settings.

METHODS

General procedure for BCP 3-alkylation

4CzIPN (PC **1**; 3.94 mg, 5.0 μmol, 0.01 equiv), copper(II)dibromide ($CuBr_2$; 22.3 mg, 0.1 mmol, 0.2 equiv), *tert*-butyl-methyl aminosilane (333.8 mg, 1.00 mmol, 2.0 equiv), and, if a solid, the limiting alkyl bromide (0.5 mmol, 1.0 equiv) were added to an oven-dried 40 mL vial equipped with a Teflon stir bar and desiccated NaOAc (82 mg, 1.0 mmol, 2.0 equiv). The vessel was closed, sealed with electrical tape, and then back filled under N_2 gas. Anhydrous, degassed acetone (10 mL, 0.05 M) was then added. If a liquid, the alkyl bromide was introduced via syringe at this step, and the vessel was placed under N_2 gas. The resultant reaction mixture was subsequently stirred within the integrated photoreactor (450 nm irradiation, 100% light intensity) for 0.5 h. After 0.5 h, the reaction mixture was opened to air and directly subjected to purification via flash chromatography, affording the desired 3-alkylated product.

General procedure for BCP 3-(hetero)arylation

$[Ir(dtbbpy)(ppy)_2]PF_6$ (PC; 4.6 mg, 5.0 μmol, 0.01 equiv), copper bis(2,2,6,6-tetramethyl-3,5-heptanedionate) ($Cu(TMHD)_2$;

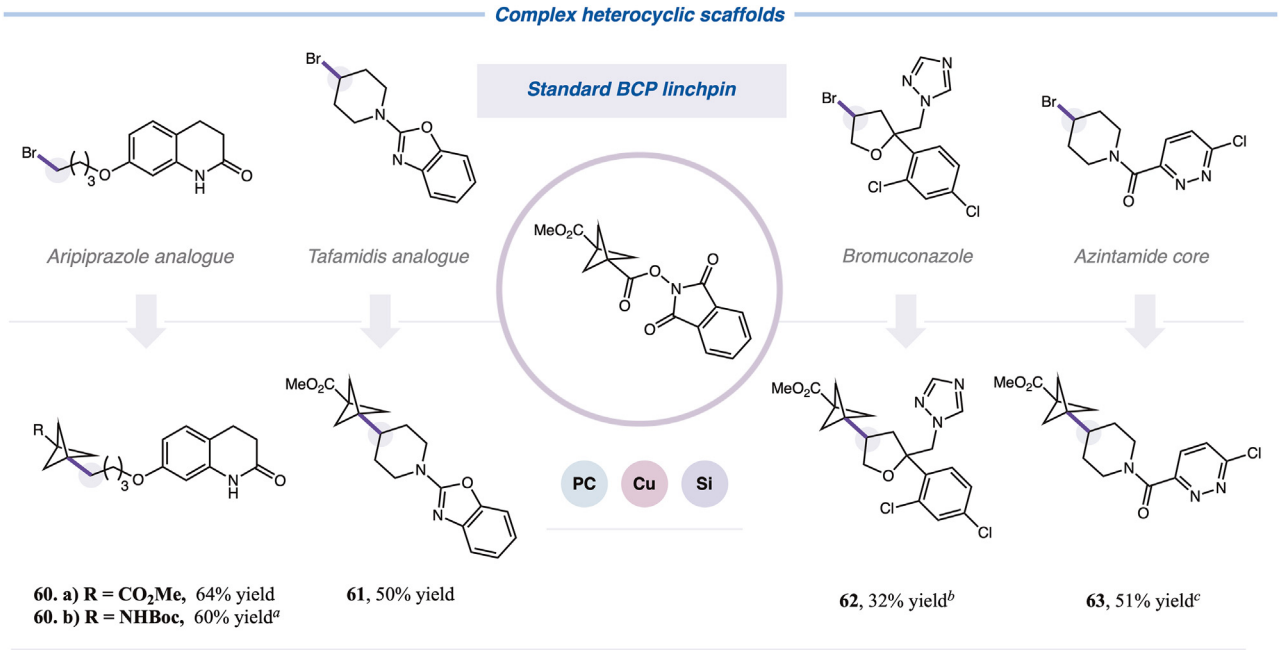

Figure 3. Applications to drug-relevant motifs

Performed according to standard alkylation procedures. Yields are isolated unless otherwise indicated. See the supplemental information for specific experimental details.

[a]Assay yield attained by ^{1}H NMR with mesitylene as the internal standard.

[b]d.r. (1.99:1) determined by liquid chromatography-mass spectrometry (LC-MS).

[c]Assay yield attained by ^{1}H NMR with TMB as the internal standard.

107.5 mg, 0.25 mmol, 0.5 equiv), (adamantylamino)supersilane (397.9 mg, 1.00 mmol, 2.0 equiv), and, if a solid, the limiting aryl bromide (0.5 mmol, 1.0 equiv) were added to an oven-dried 40 mL vial equipped with a Teflon stir bar and desiccated NaOAc (328 mg, 4.0 mmol, 8.0 equiv). The vessel was closed, sealed with electrical tape, and then back filled under N_2 gas. Anhydrous, degassed acetone (10 mL, 0.05 M) was then added. If a liquid, the aryl bromide was introduced via syringe at this step, and the vessel was placed under N_2 gas. The resultant reaction mixture was subsequently stirred within the integrated photoreactor (450 nm irradiation, 100% light intensity) for 1 h. After 1 h, the reaction mixture was opened to air and directly subjected to purification via flash chromatography, affording the desired 3-arylated product.

Selection of silane reagent

The *tert*-butyl-methyl aminosilane reagent was implemented to prevent deactivation of the NHPI redox-active ester. It is postulated that the silane reagent generates an equivalent ratio of alkyl amine according to the proposed aza-Brook rearrangement and consequently participates in undesired nucleophilic attack of the BCP NHPI reagent. The *tert*-butyl substituent provides sufficient steric hindrance to disfavor addition into the electrophilic carbon of the NHPI redox-active ester. The *tert*-butyl-methyl aminosilane can be prepared on a gram scale via a one-step protocol from commercially available starting materials. Key reagents include triflic acid, supersilane, and *N-tert*-butyl-methyl amine (1 g, US$36 at the time of writing). *Nota bene*: supersilane gives a drastically lower yield than the optimal *tert*-butyl-methyl aminosilane reagent. For further reaction optimization data and reaction details, see supplemental information sections S4–S7 and Figures S1–S31.

Other experimental details and examples, as well as characterization data, can be found in the supplemental information.

RESOURCE AVAILABILITY

Lead contact

Requests for further information and resources should be directed to and will be fulfilled by the lead contact, David W.C. MacMillan (dmacmill@princeton.edu).

Materials availability

This study did not involve the design of unique reagents or catalysts for chemical synthesis.

Data and code availability

There is no dataset or code associated with this publication. All relevant procedures and experimental data are provided in the supplemental information.

ACKNOWLEDGMENTS

Research reported in this work was supported in part by the National Institute of General Medical Sciences of the National Institutes of Health (R35GM134897) and in part by the Office of Naval Research (N000142112138). K.I.B. thanks the Ted Taylor family for an Edward C. Taylor Fellowship graduate fellowship. K.I.B. also thanks Dr. Jiaxin Xie, Dr. Nicholas Intermaggio, Dr. Christian Oswood, and

Dr. Nathan Dow for helpful conversations and Dr. Robert Martin for computational assistance. The authors thank Dr. Brandon Kennedy (Lotus Separations) for assistance with compound purification and Rebecca Lambert for assistance in preparing this manuscript.

AUTHOR CONTRIBUTIONS

D.W.C.M. and K.I.B. conceived the research; K.I.B. designed the experiments, carried out the experiments, and analyzed the results under the guidance of D.W.C.M.; and K.I.B. and D.W.C.M. prepared the manuscript.

DECLARATION OF INTERESTS

D.W.C.M. declares a competing financial interest with respect to the integrated photoreactor.

SUPPLEMENTAL INFORMATION

Supplemental information can be found online at https://doi.org/10.1016/j.chempr.2025.102537.

Received: November 6, 2024
Revised: January 16, 2025
Accepted: March 14, 2025
Published: April 8, 2025

REFERENCES

1. Veber, D.F., Johnson, S.R., Cheng, H.-Y., Smith, B.R., Ward, K.W., and Kopple, K.D. (2002). Molecular properties that influence the oral bioavailability of drug candidates. J. Med. Chem. *45*, 2615–2623. https://doi.org/10.1021/jm020017n.
2. Lovering, F., Bikker, J., and Humblet, C. (2009). Escape from Flatland: increasing saturation as an approach to improving clinical success. J. Med. Chem. *52*, 6752–6756. https://doi.org/10.1021/jm901241e.
3. Lovering, F. (2013). Escape from Flatland 2: complexity and promiscuity. Med. Chem. Commun. *4*, 515–519. https://doi.org/10.1039/C2MD20347B.
4. Meanwell, N.A. (2011). Synopsis of some recent tactical application of bioisosteres in drug design. J. Med. Chem. *54*, 2529–2591. https://doi.org/10.1021/jm1013693.
5. Meanwell, N.A. (2023). Applications of bioisosteres in the design of biologically active compounds. J. Agric. Food Chem. *71*, 18087–18122. https://doi.org/10.1021/acs.jafc.3c00765.
6. Alvarez, E.M., Bai, Z., Pandit, S., Frank, N., Torkowski, L., and Ritter, T. (2023). O-, N- and C-bicyclopentylation using thianthrenium reagents. Nat. Synth. *2*, 548–556. https://doi.org/10.1038/s44160-023-00277-8.
7. Guengerich, F.P. (2018). Mechanisms of cytochrome P450-catalyzed oxidations. ACS Catal. *8*, 10964–10976. https://doi.org/10.1021/acscatal.8b03401.
8. Bayliss, M.K., Butler, J., Feldman, P.L., Green, D.V.S., Leeson, P.D., Palovich, M.R., and Taylor, A.J. (2016). Quality guidelines for oral drug candidates: dose, solubility and lipophilicity. Drug Discov. Today *21*, 1719–1727. https://doi.org/10.1016/j.drudis.2016.07.007.
9. Stepan, A.F., Subramanyam, C., Efremov, I.V., Dutra, J.K., O'Sullivan, T.J., DiRico, K.J., McDonald, W.S., Won, A., Dorff, P.H., Nolan, C.E., et al. (2012). Application of the bicyclo[1.1.1]pentane motif as a nonclassical phenyl ring bioisostere in the design of a potent and orally active γ-secretase inhibitor. J. Med. Chem. *55*, 3414–3424. https://doi.org/10.1021/jm300094u.
10. Shire, B.R., and Anderson, E.A. (2023). Conquering the synthesis and functionalization of bicyclo[1.1.1]pentanes. JACS Au *3*, 1539–1553. https://doi.org/10.1021/jacsau.3c00014.
11. Subbaiah, M.A.M., and Meanwell, N.A. (2021). Bioisosteres of the phenyl ring: recent strategic applications in lead optimization and drug design. J. Med. Chem. *64*, 14046–14128. https://doi.org/10.1021/acs.jmedchem.1c01215.
12. Ma, X., Sloman, D.L., Han, Y., and Bennett, D.J. (2019). A selective synthesis of 2,2-difluorobicyclo[1.1.1]pentane analogues: "BCP-F2.". Org. Lett. *21*, 7199–7203. https://doi.org/10.1021/acs.orglett.9b02026.
13. Caputo, D.F.J., Arroniz, C., Dürr, A.B., Mousseau, J.J., Stepan, A.F., Mansfield, S.J., and Anderson, E.A. (2018). Synthesis and applications of highly functionalized 1-halo-3-substituted bicyclo[1.1.1]pentanes. Chem. Sci. *9*, 5295–5300. https://doi.org/10.1039/c8sc01355a.
14. Nugent, J., Arroniz, C., Shire, B.R., Sterling, A.J., Pickford, H.D., Wong, M.L.J., Mansfield, S.J., Caputo, D.F.J., Owen, B., Mousseau, J.J., et al. (2019). A general route to bicyclo[1.1.1]pentanes through photoredox catalysis. ACS Catal. *9*, 9568–9574. https://doi.org/10.1021/acscatal.9b03190.
15. Gianatassio, R., Lopchuk, J.M., Wang, J., Pan, C.-M., Malins, L.R., Prieto, L., Brandt, T.A., Collins, M.R., Gallego, G.M., Sach, N.W., et al. (2016). Organic chemistry. Strain-release amination. Science *351*, 241–246. https://doi.org/10.1126/science.aad6252.
16. Lopchuk, J.M., Fjelbye, K., Kawamata, Y., Malins, L.R., Pan, C.-M., Gianatassio, R., Wang, J., Prieto, L., Bradow, J., Brandt, T.A., et al. (2017). Strain-release heteroatom functionalization: development, scope, and stereospecificity. J. Am. Chem. Soc. *139*, 3209–3226. https://doi.org/10.1021/jacs.6b13229.
17. Makarov, I.S., Brocklehurst, C.E., Karaghiosoff, K., Koch, G., and Knochel, P. (2017). Synthesis of bicyclo[1.1.1]pentane bioisosteres of internal alkynes and para-disubstituted benzenes from [1.1.1]propellane. Angew. Chem. Int. Ed. *56*, 12774–12777. https://doi.org/10.1002/anie.201706799.
18. Zhang, X., Smith, R.T., Le, C., McCarver, S.J., Shireman, B.T., Carruthers, N.I., and MacMillan, D.W.C. (2020). Copper-mediated synthesis of drug-like bicyclopentanes. Nature *580*, 220–226. https://doi.org/10.1038/s41586-020-2060-z.
19. Ripenko, V., Sham, V., Levchenko, V., Holovchuk, S., Vysochyn, D., Klymov, I., Kyslyi, D., Veselovych, S., Zhersh, S., Dmytriv, Y., et al. (2024). Light-enabled scalable synthesis of bicyclo[1.1.1]pentane halides and their functionalizations. Nat. Synth. *3*, 1538–1549. https://doi.org/10.1038/s44160-024-00637-y.
20. Garlets, Z.J., Sanders, J.N., Malik, H., Gampe, C., Houk, K.N., and Davies, H.M.L. (2020). Enantioselective C–H functionalization of bicyclo[1.1.1]pentanes. Nat. Cat. *3*, 351–357. https://doi.org/10.1038/s41929-019-0417-1.
21. Huang, W., Zheng, Y., Keess, S., and Molander, G.A. (2023). A general and modular approach to BCP alkylamines via multicomponent difunctionalization of [1.1.1]propellane. J. Am. Chem. Soc. *145*, 5363–5369. https://doi.org/10.1021/jacs.2c13298.
22. Yu, I.F., Manske, J.L., Diéguez-Vázquez, A., Misale, A., Pashenko, A.E., Mykhailiuk, P.K., Ryabukhin, S.V., Volochnyuk, D.M., and Hartwig, J.F. (2023). Catalytic undirected borylation of tertiary C–H bonds in bicyclo[1.1.1]pentanes and bicyclo[2.1.1]hexanes. Nat. Chem. *15*, 685–693. https://doi.org/10.1038/s41557-023-01159-4.
23. Goh, Y.L., Cui, Y.T., Pendharkar, V., and Adsool, V.A. (2017). Toward resolving the resveratrol conundrum: synthesis and in vivo pharmacokinetic evaluation of BCP–resveratrol. ACS Med. Chem. Lett. *8*, 516–520. https://doi.org/10.1021/acsmedchemlett.7b00018.
24. Yang, Y., Tsien, J., Dykstra, R., Chen, S.-J., Wang, J.B., Merchant, R.R., Hughes, J.M.E., Peters, B.K., Gutierrez, O., and Qin, T. (2024). Programmable late-stage functionalization of bridge-substituted bicyclo[1.1.1]pentane bis-boronates. Nat. Chem. *16*, 285–293. https://doi.org/10.1038/s41557-023-01342-7.
25. Qin, T., Cornella, J., Li, C., Malins, L.R., Edwards, J.T., Kawamura, S., Maxwell, B.D., Eastgate, M.D., and Baran, P.S. (2016). A general alkyl-alkyl cross-coupling enabled by redox-active esters and alkylzinc reagents. Science *352*, 801–805. https://doi.org/10.1126/science.aaf6123.
26. Toriyama, F., Cornella, J., Wimmer, L., Chen, T.-G., Dixon, D.D., Creech, G., and Baran, P.S. (2016). Redox-active esters in Fe-catalyzed C–C

coupling. J. Am. Chem. Soc. *138*, 11132–11135. https://doi.org/10.1021/jacs.6b07172.

27. Polites, V.C., Badir, S.O., Keess, S., Jolit, A., and Molander, G.A. (2021). Nickel-catalyzed decarboxylative cross-coupling of bicyclo[1.1.1]pentyl radicals enabled by electron donor–acceptor complex photoactivation. Org. Lett. *23*, 4828–4833. https://doi.org/10.1021/acs.orglett.1c01558.
28. Mousseau, J.J., Perry, M.A., Bundesmann, M.W., Chinigo, G.M., Choi, C., Gallego, G., Hicklin, R.W., Hoy, S., Limburg, D.C., Sach, N.W., et al. (2022). Automated nanomole-scale reaction screening toward benzoate bioisosteres: a photocatalyzed approach to highly elaborated bicyclo[1.1.1]pentanes. ACS Catal. *12*, 600–606. https://doi.org/10.1021/acscatal.1c05076.
29. Wiesenfeldt, M.P., Rossi-Ashton, J.A., Perry, I.B., Diesel, J., Garry, O.L., Bartels, F., Coote, S.C., Ma, X., Yeung, C.S., Bennett, D.J., et al. (2023). General access to cubanes as benzene bioisosteres. Nature *618*, 513–518. https://doi.org/10.1038/s41586-023-06021-8.
30. Salgueiro, D.C., Chi, B.K., Guzei, I.A., García-Reynaga, P., and Weix, D.J. (2022). Control of redox-active ester reactivity enables a general cross-electrophile approach to access arylated strained rings. Angew. Chem. Int. Ed. *61*, e202205673. https://doi.org/10.1002/anie.202205673.
31. Yasukawa, T., Håheim, K.S., and Cossy, J. (2023). Synthesis of 1,3-disubstituted bicyclo[1.1.1]pentanes by cross-coupling induced by transition metals – formation of C–C bonds. Org. Biomol. Chem. *21*, 7666–7680. https://doi.org/10.1039/D3OB01036H.
32. DeCicco, E.M., Berritt, S., Knauber, T., Coffey, S.B., Hou, J., and Dowling, M.S. (2023). Decarboxylative cross-electrophile coupling of (hetero)aromatic bromides and NHP esters. J. Org. Chem. *88*, 12329–12340. https://doi.org/10.1021/acs.joc.3c01072.
33. Laudadio, G., Neigenfind, P., Péter, Á., Rubel, C.Z., Emmanuel, M.A., Oderinde, M.S., Ewing, T.E.-H., Palkowitz, M.D., Sloane, J.L., Gillman, K.W., et al. (2024). Nickel-electrocatalytic decarboxylative arylation to access quaternary centers. Angew. Chem. Int. Ed. *63*, e202314617. https://doi.org/10.1002/anie.202314617.
34. Zhou, J.S., and Fu, G.C. (2003). Cross-couplings of unactivated secondary alkyl halides: room-temperature nickel-catalyzed negishi reactions of alkyl bromides and iodides. J. Am. Chem. Soc. *125*, 14726–14727. https://doi.org/10.1021/ja0389366.
35. Evano, G., Wang, J., and Nitelet, A. (2017). Metal-mediated C–O bond forming reactions in natural product synthesis. Org. Chem. Front. *4*, 2480–2499. https://doi.org/10.1039/C7QO00671C.
36. Andersen, C., Ferey, V., Daumas, M., Bernardelli, P., Guérinot, A., and Cossy, J. (2020). Copper-catalyzed cross-coupling between alkyl (pseudo)halides and bicyclopentyl grignard reagents. Org. Lett. *22*, 6021–6025. https://doi.org/10.1021/acs.orglett.0c02115.
37. Le, C., Chen, T.Q., Liang, T., Zhang, P., and MacMillan, D.W.C. (2018). A radical approach to the copper oxidative addition problem: trifluoromethylation of bromoarenes. Science *360*, 1010–1014. https://doi.org/10.1126/science.aat4133.
38. Andrieux, C.P., Saveant, J.M., and Su, K.B. (1986). Kinetics of dissociative electron transfer. Direct and mediated electrochemical reductive cleavage of the carbon-halogen bond. J. Phys. Chem. *90*, 3815–3823. https://doi.org/10.1021/j100407a059.
39. Chatgilialoglu, C. (1995). Structural and chemical properties of silyl radicals. Chem. Rev. *95*, 1229–1251. https://doi.org/10.1021/cr00037a005.
40. Dow, N.W., Cabré, A., and MacMillan, D.W.C. (2021). A general N-alkylation platform via copper metallaphotoredox and silyl radical activation of alkyl halides. Chem *7*, 1827–1842. https://doi.org/10.1016/j.chempr.2021.05.005.
41. Juliá, F., Constantin, T., and Leonori, D. (2022). Applications of halogen-atom transfer (XAT) for the generation of carbon radicals in synthetic photochemistry and photocatalysis. Chem. Rev. *122*, 2292–2352. https://doi.org/10.1021/acs.chemrev.1c00558.
42. Bellotti, P., and Glorius, F. (2023). Strain-release photocatalysis. J. Am. Chem. Soc. *145*, 20716–20732. https://doi.org/10.1021/jacs.3c08206.
43. Sakai, H.A., Liu, W., Le, C.C., and MacMillan, D.W.C. (2020). Cross-electrophile coupling of unactivated alkyl chlorides. J. Am. Chem. Soc. *142*, 11691–11697. https://doi.org/10.1021/jacs.0c04812.
44. Kochi, J.K., Bemis, A., and Jenkins, C.L. (1968). Mechanism of electron transfer oxidation of alkyl radicals by copper(II) complexes. J. Am. Chem. Soc. *90*, 4616–4625. https://doi.org/10.1021/ja01019a018.
45. Faraggi, T.M., Rouget-Virbel, C., Rincón, J.A., Barberis, M., Mateos, C., García-Cerrada, S., Agejas, J., de Frutos, O., and MacMillan, D.W.C. (2021). Synthesis of enantiopure unnatural amino acids by metallaphotoredox catalysis. Org. Process Res. Dev. *25*, 1966–1973. https://doi.org/10.1021/acs.oprd.1c00208.
46. Li, Y., Zhang, Y., Wang, J., Xia, D., Zhuo, M., Zhu, L., Li, D., Ni, S.-F., Zhu, Y., and Zhang, W.-D. (2024). Visible-light-mediated three-component strategy for the synthesis of isoxazolines and isoxazoles. Org. Lett. *26*, 3130–3134. https://doi.org/10.1021/acs.orglett.4c00671.
47. Rybak, J.M., Xie, J., Martin-Vicente, A., Guruceaga, X., Thorn, H.I., Nywening, A.V., Ge, W., Souza, A.C.O., Shetty, A.C., McCracken, C., et al. (2024). A secondary mechanism of action for triazole antifungals in *Aspergillus fumigatus* mediated by *hmg1*. Nat. Commun. *15*, 3642. https://doi.org/10.1038/s41467-024-48029-2.
48. Anderson, J.M., Measom, N.D., Murphy, J.A., and Poole, D.L. (2021). Bridge functionalisation of bicyclo[1.1.1]pentane derivativess. Angew. Chem. Int. Ed. *60*, 24754–24769. https://doi.org/10.1002/anie.202106352.
49. Hiesinger, K., Dar'in, D., Proschak, E., and Krasavin, M. (2021). Spirocyclic scaffolds in medicinal chemistry. J. Med. Chem. *64*, 150–183. https://doi.org/10.1021/acs.jmedchem.0c01473.
50. Vitaku, E., Smith, D.T., and Njardarson, J.T. (2014). Analysis of the structural diversity, substitution patterns, and frequency of nitrogen heterocycles among U.S. FDA approved pharmaceuticals. J. Med. Chem. *57*, 10257–10274. https://doi.org/10.1021/jm501100b.
51. Scott, K.A., Cox, P.B., and Njardarson, J.T. (2022). Phenols in pharmaceuticals: analysis of a recurring motif. J. Med. Chem. *65*, 7044–7072. https://doi.org/10.1021/acs.jmedchem.2c00223.
52. Mao, E., Prieto Kullmer, C.N., Sakai, H.A., and MacMillan, D.W.C. (2024). Direct bioisostere replacement enabled by metallaphotoredox deoxydifluoromethylation. J. Am. Chem. Soc. *146*, 5067–5073. https://doi.org/10.1021/jacs.3c14460.
53. Ritchie, T.J., and Macdonald, S.J.F. (2009). The impact of aromatic ring count on compound developability – are too many aromatic rings a liability in drug design? Drug Discov. Today *14*, 1011–1020. https://doi.org/10.1016/j.drudis.2009.07.014.
54. Dombrowski, A.W., Gesmundo, N.J., Aguirre, A.L., Sarris, K.A., Young, J.M., Bogdan, A.R., Martin, M.C., Gedeon, S., and Wang, Y. (2020). Expanding the medicinal chemist toolbox: comparing seven $C(sp^2)$–$C(sp^3)$ cross-coupling methods by library synthesis. ACS Med. Chem. Lett. *11*, 597–604. https://doi.org/10.1021/acsmedchemlett.0c00093.
55. Meanwell, N.A. (2018). Fluorine and Fluorinated motifs in the design and application of bioisosteres for drug design. J. Med. Chem. *61*, 5822–5880. https://doi.org/10.1021/acs.jmedchem.7b01788.
56. Talele, T.T. (2016). The "cyclopropyl fragment" is a versatile player that frequently appears in preclinical/clinical drug molecules. J. Med. Chem. *59*, 8712–8756. https://doi.org/10.1021/acs.jmedchem.6b00472.